



The thermal degradation property and flame-retardant mechanism of coated knitted cotton fabric with chitosan and APP by LBL assembly

Hua-Qi Chen¹ · Ying-Jun Xu² · Zhi-Ming Jiang² · Xing Jin³ · Yun Liu² · Lin Zhang² · Chuan-Jie Zhang¹ · Chao Yan¹

Received: 23 April 2019 / Accepted: 13 September 2019 / Published online: 1 October 2019
© Akadémiai Kiadó, Budapest, Hungary 2019

Abstract

In order to improve the flame retardancy of knitted cotton fabrics and investigate the flame-retardant mechanism of the system formed by ammonium polyphosphate (APP) and chitosan (CS), flame-retardant knitted cotton fabrics coated with APP and CS were successfully prepared by layer by layer assembly. APP and CS formed the intumescent flame-retardant system, in which CS acted as the carbon source agent and APP acted as both the acid source and foaming agent. The surface micromorphologies before and after flaming of coated knitted cotton fabrics were exploited by scanning electron microscopy. The flammability, combustion behaviors, thermal degradation properties and flame-retardant mechanism of this system were investigated by vertical burning test, cone calorimetry test and thermogravimetric analysis coupled with Fourier transform infrared analysis in N₂ atmosphere, respectively. Compared with the control sample, the deposition of APP and CS endowed the knitted cotton fabrics with improved flame retardancy, higher residual chars, lower heat release rate and total heat release, while increased the smoke production. Improved flame-retardant behaviors are attributed to the thermally stable residual chars, more release of inflammable gases and potential free radical scavengers (PO·) in the gaseous products, named the combination of the condensed-phase and gaseous-phase flame-retardant mechanism.

Keywords Thermal degradation property · Flame retardancy · Flame-retardant mechanism · LBL assembly

Introduction

As one of the most popular natural fibers in industry and our daily life, cotton fibers have the advantages of good sweat absorption, soft feel, easy cleaning, not easy to pilling, moisturizing, heat resistance, alkali resistance, hygiene and so on [1, 2]. However, the limiting oxygen

index (LOI) value of cotton fabrics is only about 18.4%, which makes it easy to be ignited and greatly limits its broader applications [3]. Therefore, it is of great significance to improve the flame retardancy of cotton fabrics. By now, various methods such as traditional pad-dry-cure [4], plasma [5], UV-curable [6, 7], sol-gel treatment [8, 9] and layer by layer (LBL) assembly [10–13] have been developed to build a flame-retardant coating on cotton fabrics. In recent years, layer compounds and compounds containing flame-retardant elements were synthesized to apply in the field of flame retardancy [14–18]; however, they were not widely used in flame-retardant cotton fabrics. Among these methods, the layer by layer (LBL) assembly has attracted extensive attentions from researchers [10–13]. The preparation process of LBL assembly is simple and convenient for fabricating functional, multilayer and thin films [19]. This technique utilizes the principle of alternate layer deposited by positive and negative electrolytes [20]. It is a technique that can effectively build a flame-retardant coating on the surface of a polymeric material.

✉ Yun Liu
liuyun0215@126.com

✉ Chao Yan

¹ College of Chemistry and Chemical Engineering, Hubei Key Laboratory of Biomass Fibers and Eco-dyeing and Finishing, Wuhan Textile University, Fangzhi Road, 1, Wuhan 430073, China

² College of Textiles and Clothing, Institute of Functional Textiles and Advanced Materials, Qingdao University, Ningxia Road, 308, Qingdao 266071, China

³ Tianjin Fire Research Institute of the Ministry of Emergency Management, Tianjin 300381, China

Due to the amine protonation, chitosan (CS), acquired from *N*-deacetylation of chitin, can form positive charges in dilute acid solutions [21]. Therefore, CS can be used as the polycation in LBL assembly [22, 23]. In the recent researches, CS has been utilized to flame retard foams [24, 25], nylon fabrics [26], and cellulose fabrics [27–29] by LBL assembly. It is noted that the flame retardancy of cotton fabrics can be obviously promoted combining CS with phosphorus-containing compounds through LBL assembly. These compounds containing phosphorus include phosphorylated poly (vinyl alcohol) (PPVA) [28], phosphorylated chitin [29], sodium phytate [21], ammonium polyphosphate (APP) [27, 30, 31], and so on. APP, a kind of phosphorus-containing compound, is one of the most commonly used inorganic flame retardant [32–34] and can form negative charges in aqueous solutions. As a result, APP can be utilized as the polyanion in LBL assembly to prepare flame-retardant cotton fabrics [35]. In the previous researches, the results indicate that the flame-retardant properties of the cotton fabrics coated with APP and polyhexamethylene guanidine phosphate (PHMGP) [36], polyethyleneimine (BPEI) [37], sodium montmorillonite (MMT) [38], and vinyltrimethoxysilane (VTMS) [38] are obviously improved, respectively.

CS has many reactive hydroxyl groups [21] and can be used as a carbon source to form the intumescent flame retardant with APP. Recently, the thermal stability properties and flame retardancy of cotton fabrics coated with APP and CS through LBL assembly were investigated [27]. The results indicate that the coating with APP and CS can greatly reduce the values of peak heat release rate (PHRR) and total heat release (THR) obtained from microscale combustion calorimetry (MCC) test, and the afterflame time in the vertical burning test. However, the coated cotton fabrics with 14.3 mass% add-on cannot pass the vertical burning test. In addition, CS/APP, silica/APP and CS/APP/silica coating system on PET-CO blends were also investigated [30, 31]. The results show that the suppression of the afterglow phenomenon after the LBL assembly can be obtained. However, the PET-CO fabrics with 20 BL coatings still failed in the vertical burning test, and the flame-retardant mechanism of coated cotton fabrics with APP and CS is not explored in the papers mentioned above.

In order to prepare flame-retardant cotton fabrics with APP/CS coating passing the vertical burning test and understand the flame-retardant mechanism of this system, the coated knitted cotton fabrics were successfully prepared with APP and CS through LBL assembly. Before APP and CS coating, the knitted cotton fabrics were dipped into 3-aminopropyl triethoxysilane (APTES) aqueous solutions to endow the surface of the fabrics with positive charges. The structure, micromorphologies, thermal stabilities, flame-retardant properties, combustion properties

and flame-retardant mechanism of coated knitted cotton fabrics were investigated by Fourier transform infrared analysis (FTIR), scanning electron microscopy (SEM), thermogravimetric analysis coupled with Fourier transform infrared analysis (TG-FTIR), vertical burning test, and cone calorimetry test.

Experimental

Materials

Knitted cotton fabrics (160 g m^{-2}) were supplied by Shanghai Challenge Textile Co., Ltd. (Shanghai, China). APTES was purchased from Aladdin Industrial Co. Ltd. (Shanghai, China). APP was obtained from Shifang Taifeng New Flame Retardant Co., Ltd. (Shifang, China). CS with a deacetylation degree of 95–100% was obtained from Shanghai Luna Biological Technology Co., Ltd. (Shanghai, China). The sulfuric acid and glacial acetic acid were provided by Sinopharm chemical Reagent Co., Ltd. (Tianjin, China). All the reagents were used as received.

Preparation of flame-retardant knitted cotton fabrics

In order to remove the dust on the surface of knitted cotton fabrics, the substrates were washed in deionized water and dried at $100 \text{ }^\circ\text{C}$. Then, the knitted cotton fabrics were dipped into 1 mass% APTES aqueous solution at $40 \text{ }^\circ\text{C}$ for 5 min, dried in an oven at $100 \text{ }^\circ\text{C}$, and this sample was named as the control sample. And then, the treated knitted cotton fabrics were alternately immersed into 1 mass% APP aqueous solutions and 0.5 mass% chitosan aqueous solutions, respectively. The immersion process for each step was set to be 5 min to promote and achieve a uniform deposition. After each immersion step, the coated knitted cotton fabrics were dried in the oven at $100 \text{ }^\circ\text{C}$. The coated knitted cotton fabrics were weighed after each bilayer. The process was repeated until the mass gain of the fabrics reached 6.0 mass%, 10.1 mass%, 16.6 mass% in each system.

Measurements

Cone calorimetry

According to ISO 5660-1 standard, the specimens with $100 \text{ mm} \times 100 \text{ mm}$ were wrapped in the aluminum foil, and put in a metallic grid holder. The combustion behaviors of the control sample and coated knitted cotton fabrics were investigated under a 35 kW m^{-2} heat flux horizontal. This test was carried out by a cone calorimetry (Fire Testing Technology, UK). Each sample was tested for three times.

TG-FTIR in N₂

In order to investigate the thermal decomposition behaviors of the control and coated knitted cotton fabrics, a TG analyzer (PerkinElmer STA 6000) coupled with an FTIR spectrometer (PerkinElmer Frontier FTIR) was employed. In a nitrogen atmosphere with a flow rate of 50 mL min⁻¹, 10 ± 0.2 mg of each sample was heated to 710 °C at a rate of 10 °C min⁻¹. The gaseous compounds released during the thermal degradation process were input to the FTIR gas cell. The spectral range of FTIR spectrometer was from 4000 to 450 cm⁻¹ with a 2 cm⁻¹ resolution. A stainless steel pipe was used to link the TG analyzer and the FTIR spectrometer which was equipped with the gas cell. The stainless steel pipe and the gas cell were maintained at 280 °C to avoid tar condensation of volatile products generated during the pyrolysis process and minimize secondary reactions.

SEM

The micromorphologies of the control and coated knitted cotton fabrics before and after flaming were analyzed by scanning electron microscope (SEM, vega3, TESCAN, Czech). The samples before test were coated with gold and photographed at an accelerating voltage of 10 kV.

Vertical burning test

The research of flame-retardant properties of the control sample and coated knitted cotton fabrics were exploited by a vertical burning instrument (CZF-2 typed, Jiangning, China). According to GB/T 5455-1997, the cotton fabrics were cut to 80 mm × 300 mm. A propane burner was used to ignite the spacemen for 12 s from the bottom, and the length of the flame for the igniter was 40 ± 2 mm. The whole burning process was recorded by a digital video recorder.

ATR-FTIR

An attenuated total reflectance Fourier transform infrared (ATR-FTIR) spectroscopy was recorded by a Nicolet iS 50 FTIR spectrometer (Thermo Fisher Scientific, USA) using 32 scans in the frequency region of 4000–500 cm⁻¹. The resolution was about 2.0 cm⁻¹.

Results and discussion

Structure of flame-retardant knitted cotton fabrics

An ATR-FTIR spectroscopy was utilized to explore the characteristic groups on the surface of the control and

coated knitted cotton fabrics. Figure 1 plots the ATR-FTIR spectra of the control and knitted cotton fabrics coated with APP and CS. The bands of the control sample at about 3330 and 3271 cm⁻¹ are ascribed to –O–H and –NH₂ stretching vibration, which are overlapped; the peaks at about 2898 cm⁻¹ are attributed to –CH₂– stretching vibration; the bands at about 1635 and 1518 cm⁻¹ are due to the –NH₂ and –NH₃⁺ bending vibration, respectively; the bands at 1426 and 1314 cm⁻¹ are assigned to –CH₂– deformation vibrations and C–H bending vibrations, respectively; the peak at about 1106 cm⁻¹ is ascribed to Si–O stretching vibration; the peaks at 1157 and 1028 cm⁻¹ are due to C–O–C antisymmetrical bridge stretching and stretching vibrations, respectively. Due to the polysaccharide nature of cellulose and CS, the signals of CS are not obvious from those of cotton; however, some typical signals of APP can be obtained. The typical absorption peaks of APP include 1256 cm⁻¹ (P=O), 1075 cm⁻¹ (P–O symmetric stretch) and 880 cm⁻¹ (P–O asymmetric stretch) [39]. The peaks at 892 cm⁻¹ appeared on coated knitted cotton fabrics are attributed to P–O–P stretching vibration of APP [40]. It is worth noting from Fig. 1 that the peaks between 3440 and 2700 cm⁻¹ overlap in a single signal with increasing the number of BL. The appearance of P–O–P groups for coated knitted cotton fabrics shows that APP was successfully deposited on the surface of knitted cotton fabrics.

Surface micromorphologies of flame-retardant knitted cotton fabrics

In order to assess the micromorphologies of the flame-retardant knitted cotton fabrics, SEM observations had

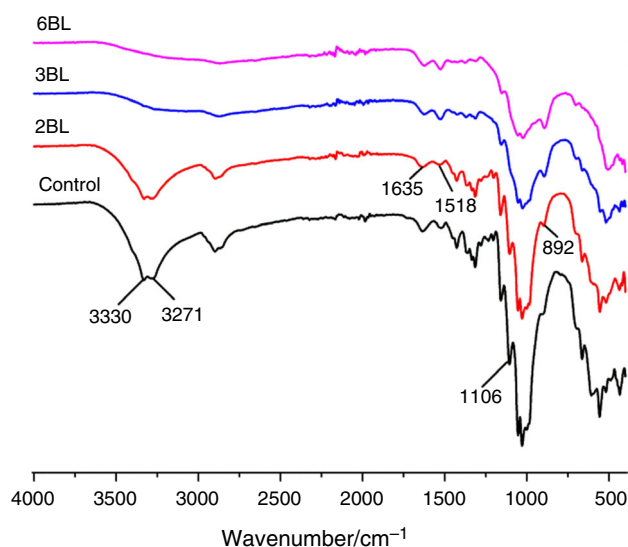
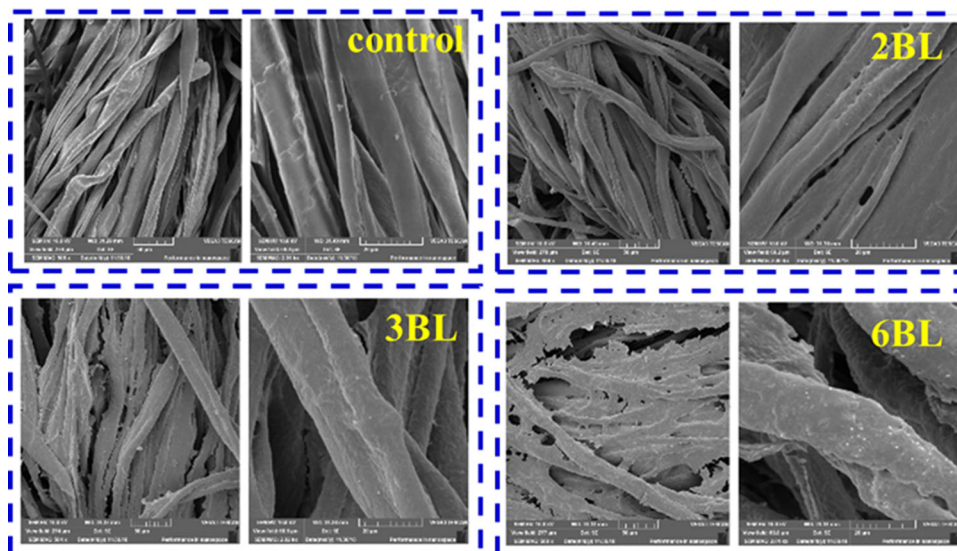


Fig. 1 ATR-FTIR spectra of the control and coated knitted cotton fabrics

Fig. 2 SEM images of control and coated knitted cotton fabrics at different magnification ($\times 500$, $\times 2000$) before burning



been performed. Some SEM images of the control and coated knitted cotton fabrics at different magnifications ($\times 500$, $\times 2000$) are collected in Fig. 2. First of all, it can be observed that the typical micromorphology of the control sample exhibits smooth and clean. When 2 APP/CS bilayers are deposited on the knitted cotton fabrics, the surface of the fibers still appears quite smooth and clean obtained from the 2000 magnification. However, the surfaces of flame-retardant knitted cotton fibers exhibit rougher when the bilayers increase to 3BL and 6BL because the coating covers the cotton fibers completely. The gaps among cotton fibers vanished because of the increasing amount of the coatings, and the add-ons of 2BL, 3BL and 6BL are 6.0 mass%, 10.1 mass% and 16.6 mass%, respectively. It is worth noting that there are no cracks in the thickness and stiffness coatings attributed to the fine and homogeneous dispersion of APP and CS.

Thermal stabilities of flame-retardant cotton fabrics

In order to investigate the thermal decomposition behaviors of the systems, a thermogravimetric analysis coupled with FTIR in nitrogen was utilized. Figure 3 displays the TGA and DTG curves of the control and coated knitted cotton fabrics, and the obtained data are summarized in Table 1. One step can be observed for the thermal degradation of the control sample, which occurs between 247 and 426 °C. During this stage, about 70% mass losses, which is ascribed to the degradation of saccharide rings for cotton fibers to produce glucose and further broken down into smaller molecular volatiles and residual chars [41]. At the end of the test, the residual char is 20.4% remaining. All the coated knitted cotton fabrics display the similar one step of the thermal degradation behaviors to the control sample.

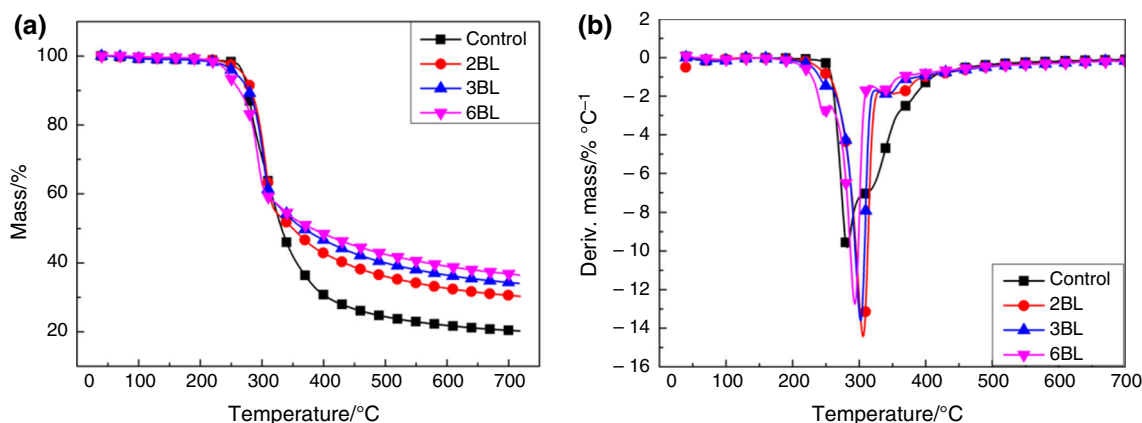


Fig. 3 TGA (a) and DTG (b) curves of control and coated knitted cotton fabrics

Table 1 Data from TGA and DTG curves for control and coated knitted cotton fabrics in N₂

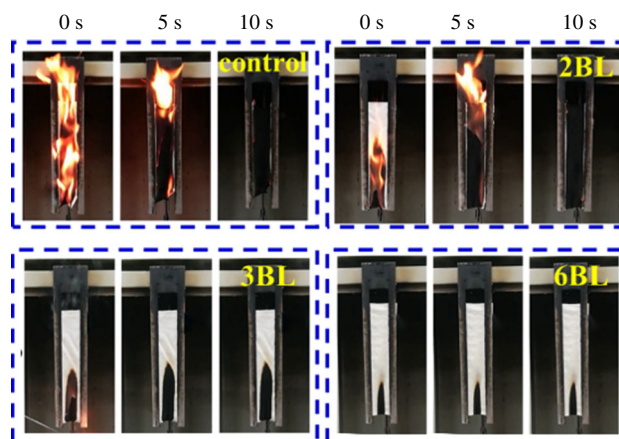
Samples	$T_{5\%}/^{\circ}\text{C}$	$T_{10\%}/^{\circ}\text{C}$	$T_{\text{max}}/^{\circ}\text{C}$	$R_{\text{max}}/\% \text{ } ^{\circ}\text{C}^{-1}$	Residues at 700 $^{\circ}\text{C}/\%$
Control	269	277	282	9.8	20.4
2BL	269	283	306	14.4	30.6
3BL	257	278	303	13.6	34.3
6BL	244	263	293	12.7	36.8

However, the thermal stability with respect to $T_{5\%}$ s is reduced, which is attributed to the earlier decomposition of APP and CS. The $T_{5\%}$ s and the maximum decomposition temperatures (T_{max} s) decrease consequently by increasing the coating amount of APP and CS, which is agreement with the results of Alongi group's work [31]. These flame-retardants containing nitrogen and/or phosphorus generally show lower thermal stability than the matrix, and decompose in advance to produce the residual char to protect the matrix from heat/mass transfer. It can be observed from Fig. 3 and Table 1 that the residual chars at higher temperature zone increase with the increment of the APP/CS coating. Polyphosphoric acid produced from the decomposition of APP can catalyze cellulose and CS containing lots of hydroxyl groups to promote residual char formation. And the higher residual char is useful to retard the heat/mass transfer between the matrix and the surrounding [41].

Flammability and combustion behaviors of flame-retardant knitted cotton fabrics

Flammability versus vertical burning test

The flame retardancy of the control and the coated knitted cotton fabrics was assessed by the vertical burning test. The obtained corresponding data are presented in Table 2, the digital images of the control and the coated knitted cotton fabrics during vertical burning tests are displayed in Fig. 4, and the SEM images of the residual char after vertical burning tests are listed in Fig. 5. The control sample completely combusted, and its afterflame and afterglow time are 14 and 0 s, respectively. And the residual char of the control sample after the vertical burning test retained. Compared with the results of our previous study [21] and Hu group's work [41], there is no afterglow phenomenon for the control sample which was treated by APTES. And

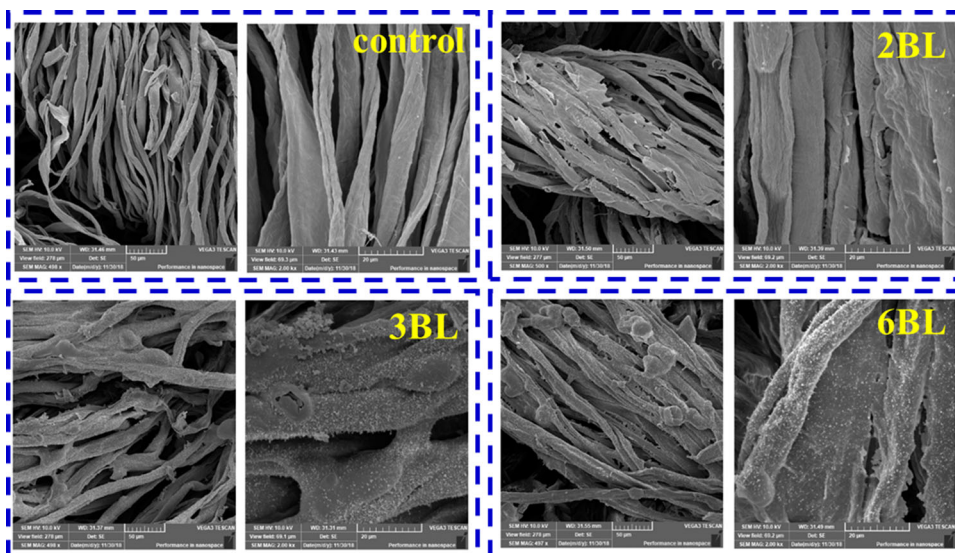
**Fig. 4** Snapshots during vertical burning test of control and coated knitted cotton fabrics recorded at 0, 5, and 10 s

this result indicates that the coating of APTES improves the flame retardancy of the cotton fabrics. 6.0 mass% deposition of APP and CS on the surface of fibers still cannot prevent the fire spread, however, the residual char completely retained. When the deposition amount of APP and CS increased to 10.1 mass%, the knitted cotton fabrics exhibit good flame retardancy, and the flame extinguishes after burning for 2 s. Moreover, the knitted cotton fabrics with 16.6 mass% deposition of APP and CS emerge better flame retardancy, and the flame extinguished immediately when the fire igniter was removed. Polyphosphoric acid formed from the thermal decomposition of APP catalyzes the dehydration and carbonization of cotton fabrics, reducing the release amount of combustible gases and producing more amount of residual char. The residual chars protect the matrix from heat/mass transfer, thus improving the flame retardancy of the coated knitted cotton fabrics [27, 31].

Table 2 Data obtained from vertical burning test

Sample	Afterflame time/s	Afterglow time/s	Damaged length/mm
Control	14	0	300
2BL	13	0	300
3BL	2	0	166
6BL	0	0	89

Fig. 5 SEM images of char residues for control and coated knitted cotton fabrics at different magnification ($\times 500$, $\times 2000$) after vertical burning test



The micromorphologies of residual char after the vertical burning test were investigated by SEM, as shown in Fig. 5. The surface of the remained fibers in 3BL and 6BL seems very rough, and there are lots of bubbles and intumescent residual chars on the surface of fibers. These phenomena result from the intumescent effect of CS and cellulose containing a great number of hydroxyl groups as the char agent and phosphorus- and nitrogen-containing APP as the acid agent and gas agent. And some of the inert gas released from APP was trapped in the residual chars, so bubbles were formed on the surface of fibers [38]. When cotton fibers coated with APP and CS were on fire, they formed intumescent chars to prevent the matrix from further burning, thus improve flame retardancy of coated knitted cotton fabrics.

Combustion properties versus cone calorimetry (cone)

The combustion properties of the control and coated knitted cotton fabrics were assessed by a cone calorimetry, the corresponding data collected are summarized in Table 3.

Figure 6a and b displays the heat release rate (HRR) and total heat release (THR) curves of the control and the coated knitted cotton fabrics as a function of time. It is worthy to note that the HRR and THR values of 2BL, 3BL and 6BL are much lower than these of the control sample. Compared with the control sample, the peak HRR (pHRR) values of 2BL, 3BL and 6BL are reduced by 44%, 56% and 75%, respectively; and THR values are decreased by 20%, 37% and 40%, respectively. In addition, the time-to-ignition (TTI) values increased with the increase in the coating amount of APP and CS. This is attributed to the compact coatings which are able to protect the matrix during the early stage of the combustion process. And the formation

of the residual chars during the combustion process further protected the matrix from heat/mass transfer, thus fewer flammable gases attended the combustion. As a result, the THR values, average HRR (Av-HRR) values and the fire growth rate indexes (FIGRA, defined as pHRR divided by TpHRR [42]) of the coated knitted cotton fabrics were sharply reduced, while the residual chars at the end of the combustion obviously increased. The results mentioned above indicate that APP and CS have an obvious effect on delaying the combustion of the knitted cotton fabrics.

Figure 7a–d presents the smoke production rate (SPR), total smoke production (TSP), CO₂ production (CO₂P), and CO production (COP) curves. It can be observed that the coating of APP and CS has a positive effect on the smoke production of the coated knitted cotton fabrics, and the results are accordant with Alongi group's work [31]. The flame-retardant effect of APP and CS prevented the knitted cotton fabrics from complete combustion, thus resulted in the release of SPR, TSP and COP and obvious decrease of CO₂P. The effective heat of combustion (EHC) is an important parameter to evaluate the heat emission from combustion of the gaseous compounds of the flammable materials [43]. Herein, the average EHC (Av-EHC) values of coated knitted cotton fabrics were lower than that of the control sample. The lower EHC and higher smoke production indicate that the more inflammable gaseous compounds appear in the gaseous phase [43].

FTIR analysis of the thermal decomposition products in gaseous phase

From the results of vertical burning test and cone calorimetry test, APP and CS present the flame inhibition in the gaseous phase and physical barrier effect in

Table 3 Data obtained from cone test

Sample	pHRR/ kW m ⁻²	TpHRR/s	Av-HRR/ kW m ⁻²	TTI/s	FIGRA/ kW m ⁻² s ⁻¹	pSPR/ m ² s ⁻¹	TSP/m ²	Av-EHC/ MJ kg ⁻¹	THR/ MJ m ⁻²	Residue/%
Control	157	60	27	25	5.8	0.007	0.45	14.92	7.3	10.5
2BL	87	50	22	29	4.0	0.013	0.41	12.08	5.8	19.9
3BL	69	55	18	42	3.8	0.020	0.62	12.43	4.6	33.2
6BL	39	55	18	46	2.2	0.020	0.55	10.88	4.4	40.0

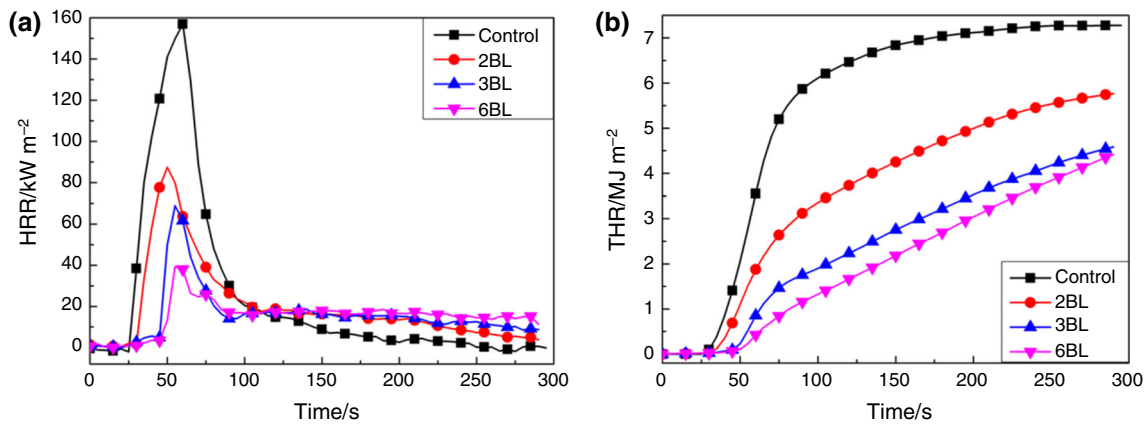


Fig. 6 HRR (a) and THR (b) curves of control and coated knitted cotton fabrics as a function of time

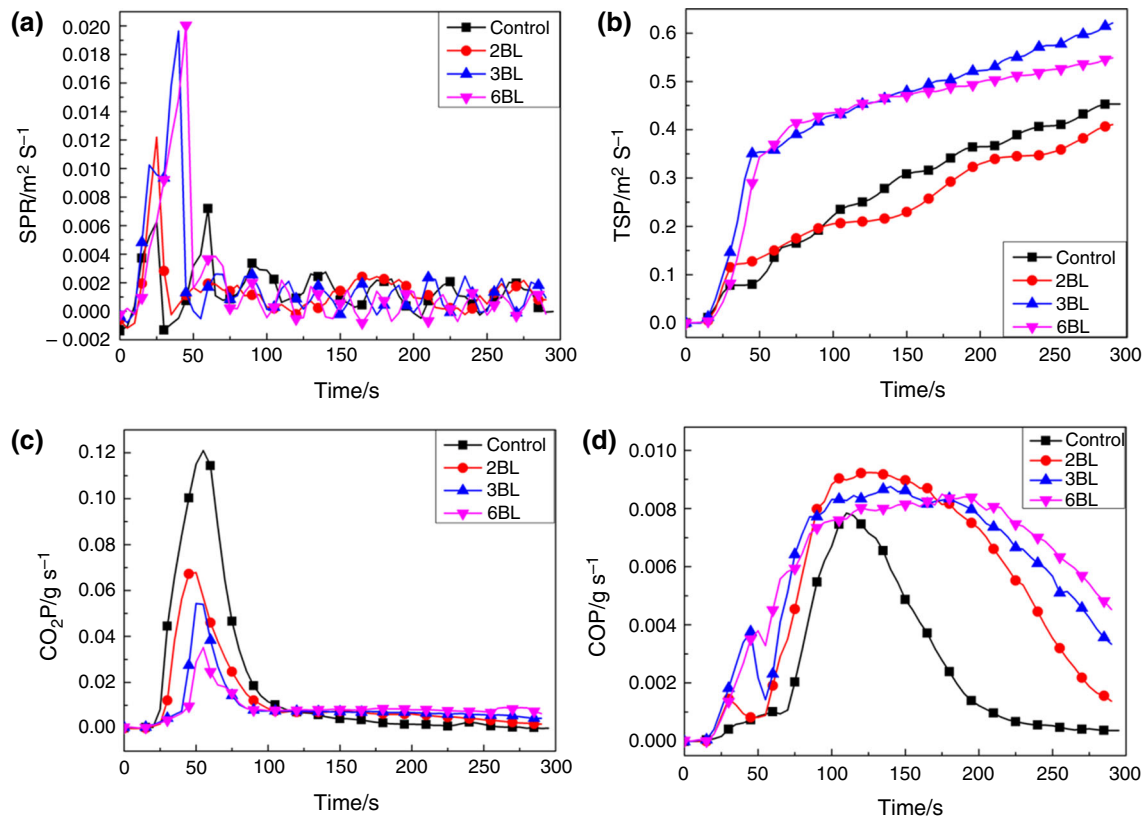


Fig. 7 SPR (a), TSP (b), CO₂P (c) and COP (d) curves of control and coated knitted cotton fabrics as a function of time

Fig. 8 3D photographs of the gaseous compounds during the thermal degradation process of the control and coated knitted cotton fabrics

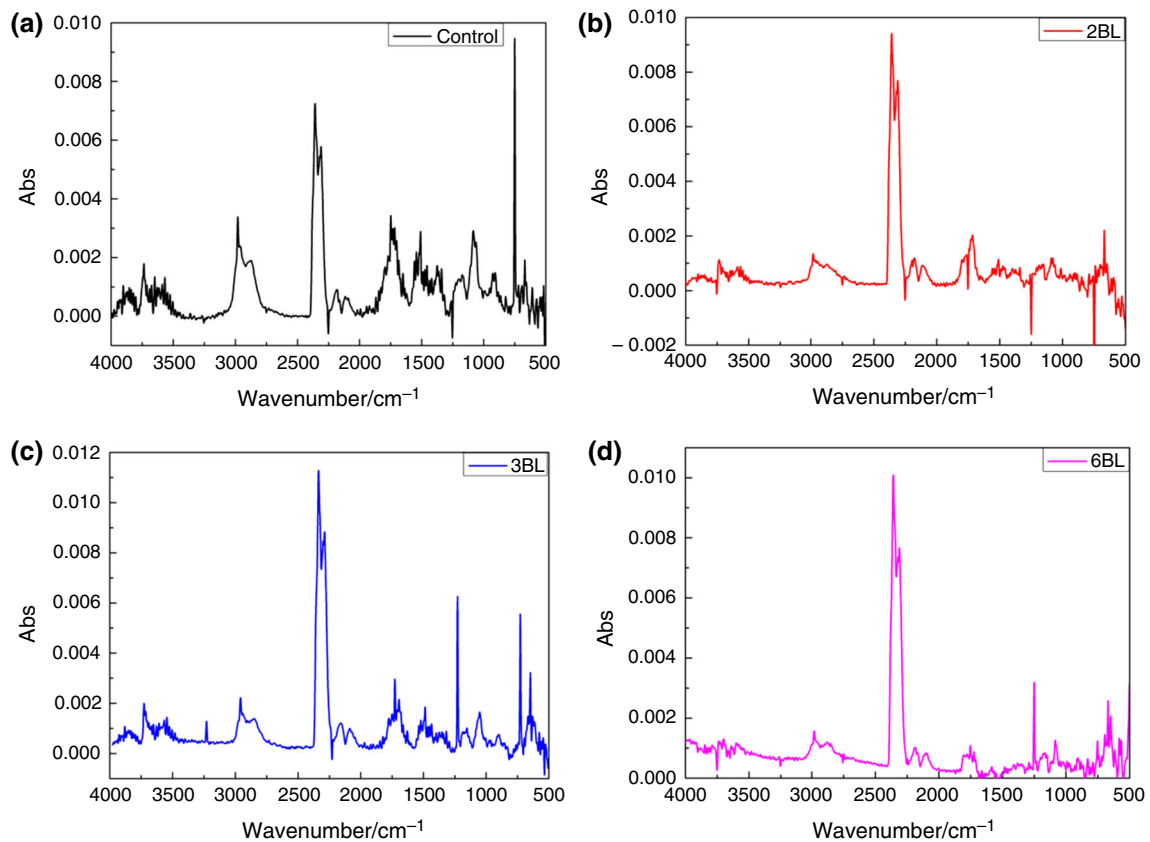
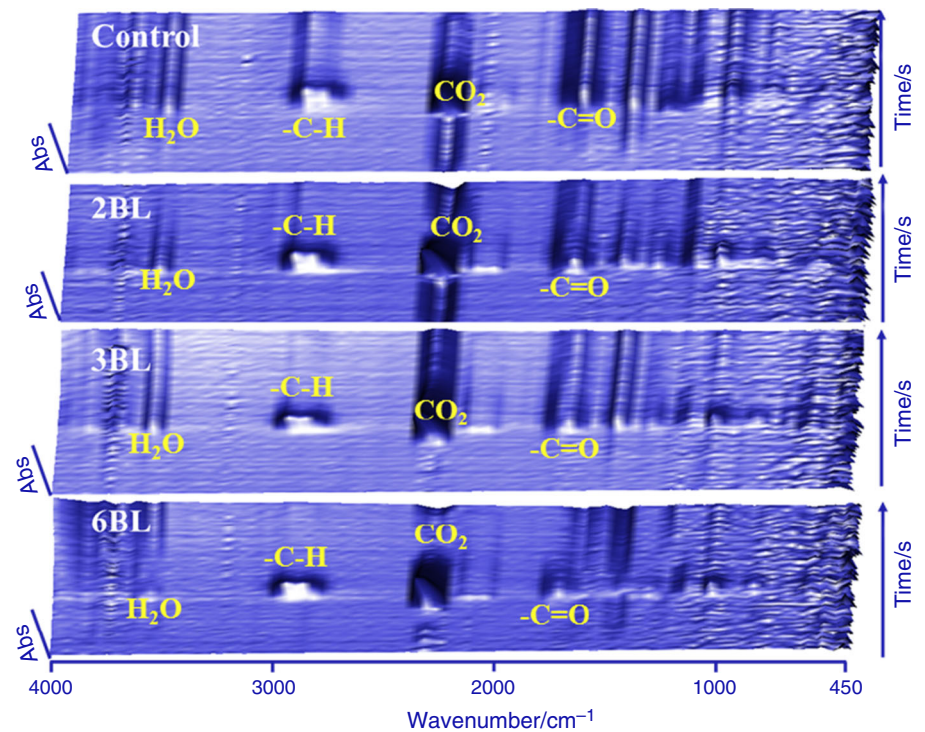


Fig. 9 FTIR spectra of samples studied at T_{\max} values

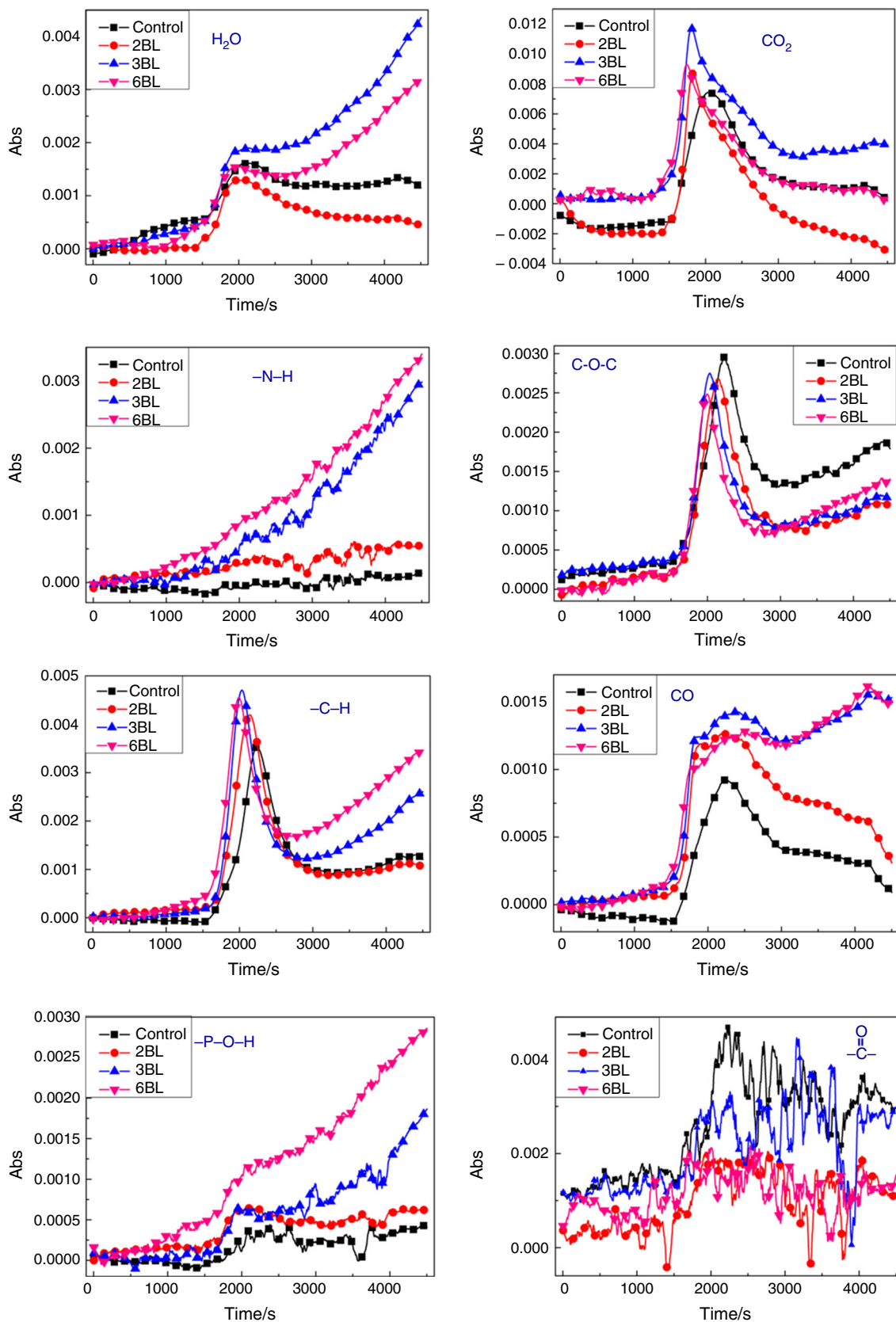


Fig. 10 Absorption intensities of chosen peaks for thermal degradation compounds of samples studied

condensed phase to flame retard knitted cotton fabrics, respectively. To further prove our supposition, the gaseous compounds formed in the thermal degradation process of the control and coated knitted cotton fabrics were explored by TG-FTIR test. 3D photographs and FTIR spectra at T_{\max} values of the control and coated knitted cotton fabrics are presented in Figs. 8 and 9. The peaks at about 3737 cm^{-1} are attributed to the stretching vibration of gaseous water and -O-H from gaseous organic chemicals; peaks from 3062 to 2782 cm^{-1} are assigned to the stretching vibration of all kinds of -C-H bonds; the bonds at about 2360 and 2308 cm^{-1} are due to the stretching vibration of CO_2 ; the peaks at about 2185 and 2107 cm^{-1} are attributed to the stretching vibration of CO ; the bond at about 1750 cm^{-1} is attributed to the stretching vibration of -C=O groups; the peak at about 1505 cm^{-1} is ascribed to the bending vibration of N-H ; the bond at about 1082 cm^{-1} is due to the stretching vibration of C-O-C groups; and the sharp peak at about 750 cm^{-1} is attributed to the bending vibration of $(\text{-CH}_2\text{-})_n$ [43]. Compared with the control sample, some new peaks appear in the FTIR spectra of coated knitted cotton fabrics. The new peak at about 3228 cm^{-1} is ascribed to the stretching vibration of N-H bond, and the peak at about 1240 cm^{-1} is due to the stretching vibration of P=O [44]. It can be obtained from Figs. 8 and 9 that the ratio values of $\gamma_{\text{-C-H}}/\gamma_{\text{CO}_2}$, $\gamma_{\text{-C=O}}/\gamma_{\text{CO}_2}$ and $\gamma_{\text{C-O-C}}/\gamma_{\text{CO}_2}$ (defined as the absorption intensities of -C-H , -C=O and C-O-C bands divided by the absorption intensity of CO_2 , respectively) for the coated knitted cotton fabrics are much lower than that of the control sample. According to the Lambert–Beer law, the relationship between the concentration of a gaseous compound and the absorption intensity of a specific wavenumber is linear [45]. Consequently, the coatings of APP and CS reduced the concentration of gaseous compounds contained the -C-H , -C=O and C-O-C groups (flammable gases) in the gaseous phase at T_{\max} s, thus suppressed the burning of the knitted cotton fabrics.

To further explore the flame-retardant mechanism of coated knitted cotton fabrics with APP and CS, eight FTIR spectra of special groups including H_2O , C-H bond, CO_2 , CO , C-O-C groups, N-H bond, P-O-H bond and C=O groups versus time are depicted in Fig. 10. The wavenumbers of chosen peaks are presented as follows: H_2O , 3737 cm^{-1} ; N-H , 3254 cm^{-1} ; C-H , 2982 cm^{-1} ; P-O-H , 2756 cm^{-1} ; CO_2 , 2362 cm^{-1} ; CO , 2183 cm^{-1} ; C=O , 1753 cm^{-1} and C-O-C , 1083 cm^{-1} . The absorption intensities of H_2O , CO_2 , -N-H and -P-O-H for 3BL and 6BL, the inflammable gases, are higher than those of the control sample; while the absorption intensities of C=O and C-O-C groups, the flammable gases, are lower than those of the control sample. However, the absorption intensities

of CO and C-H (the flammable gases) for coated knitted cotton fabrics are higher than those of the control sample.

Figures 9 and 10 show that the appearances of N-H , P=O and P-O-H bonds indicate the formation of ammonia and phosphorus-containing compounds in the gas phase. On one hand, the NH_3 , a kind of inflammable gas, can dilute the flammable gases and reduce the content of the flammable gases; on the other hand, P=O and P-O-H groups are the flame inhibitor and potential free radical scavenger source in the gas phase. The reduction of the content for the flammable gases and the flame inhibitor decreases the “fuel” to support the flame, thus improving the flame retardancy of coated knitted cotton fabrics. In addition, the intumescent chars formed (shown in Fig. 5) protect the matrix from heat/mass transfer, showing in the condensed-phase flame-retardant mechanism. As a result, the flame-retardant properties of coated knitted cotton fabrics are dramatically improved.

Conclusions

Flame-retardant knitted cotton fabrics coated with APP and CS were successfully prepared through LBL assembly. The thermal stability at higher temperature, flame retardancy, combustion behaviors is improved by the deposition of APP and CS according to the results of TGA, vertical burning and cone calorimetry tests. The formed intumescent chars protected the matrix from heat/mass transfer in the condensed phase. In the gas phase, P=O and P-O-H groups were the flame inhibitor and potential free radical scavenger source; moreover, inflammable gases such as NH_3 , H_2O , and CO_2 produced by the flame-retardant coating diluted flammable gases such as CO and C-H . Therefore, the flame-retardant properties of coated knitted cotton fabrics were improved; the flame retardancy of APP and CS coated knitted cotton fabrics was attributed to the combination of the condensed- and gaseous-phase flame-retardant mechanism. The results of this work can help to further design effective LBL assembly systems for the flame-retardant cellulosic fabrics.

Acknowledgements This work was financially supported by the National Key Research and Development Program of China (Project No. 2017YFB0309001), the National Natural Science Foundation of China (Grant No. 51673153) and Tianjin Fire Research Institute of the Ministry of Emergency Management (Grant No. KFKT2016MS02).

References

1. Montagut AM, Granados A, Ballesteros A, Pleixats R, Llagostera M, Cortés P, Sebastián RM, Vallribera A. Antibiotic protected

- silver nanoparticles for microbicidal cotton. *Tetrahedron*. 2019;75:102–8.
2. Xu QB, Zheng WS, Duan PP, Chen JN, Zhang YY, Fu FY, Diao HY, Liu XD. One-pot fabrication of durable antibacterial cotton fabric coated with silver nanoparticles via carboxymethyl chitosan as a binder and stabilizer. *Carbohydr Polym*. 2019;204:42–9.
 3. Ghoranneviss M, Shahidi S. Flame retardant properties of plasma pretreated/metallic salt loaded cotton fabric before and after direct dyeing. *J Fusion Energy*. 2014;33:119–24.
 4. Zhou L, Liang Z, Li R, Huang D, Ren X. Flame-retardant treatment of cotton fabric with organophosphorus derivative containing nitrogen and silicon. *J Therm Anal Calorim*. 2016;128:653–60.
 5. Edwards B, El-Shafei A, Hauser P, Malshe P. Towards flame retardant cotton fabrics by atmospheric pressure plasma-induced graft polymerization: synthesis and application of novel phosphoramidate monomers. *Surf Coat Technol*. 2012;209:73–9.
 6. Xing WY, Song L, Hu Y, Zhou S, Wu K, Chen LJ. Thermal properties and combustion behaviors of a novel UV-curable flame retarded coating containing silicon and phosphorus. *Polym Degrad Stab*. 2009;94:1503–8.
 7. Xing W, Jie G, Song L, Hu S, Lv X, Wang X, Hu Y. Flame retardancy and thermal degradation of cotton textiles based on UV-curable flame retardant coatings. *Thermochim Acta*. 2011;513:75–82.
 8. Alongi J, Colleoni C, Malucelli G, Rosace G. Hybrid phosphorus-doped silica architectures derived from a multistep sol-gel process for improving thermal stability and flame retardancy of cotton fabrics. *Polym Degrad Stab*. 2012;97:1334–44.
 9. Rosace G, Castellano A, Trovato V, Iacono G, Malucelli G. Thermal and flame retardant behaviour of cotton fabrics treated with a novel nitrogen-containing carboxyl-functionalized organophosphorus system. *Carbohydr Polym*. 2018;196:348–58.
 10. Pan Y, Wang W, Liu L, Ge H, Song L, Hu Y. Influences of metal ions crosslinked alginate based coatings on thermal stability and fire resistance of cotton fabrics. *Carbohydr Polym*. 2017;170:133–9.
 11. Laufer G, Kirkland C, Morgan AB, Grunlan JC. Intumescent multilayer nanocoating, made with renewable polyelectrolytes, for flame-retardant cotton. *Biomacromol*. 2012;13:2843–8.
 12. Li YC, Schulz J, Mannen S, Delhom C, Condon B, Chang SC, Zammarrano M, Grunlan J. Flame retardant behavior of polyelectrolyte-clay thin film assemblies on cotton fabric. *ACS Nano*. 2010;4:3325–37.
 13. Carosio F, Fontaine G, Alongi J, Bourbigot S. Starch-based layer by layer assembly: efficient and sustainable approach to cotton fire protection. *ACS Appl Mater Interfaces*. 2015;7:12158–67.
 14. Kong Q, Wu T, Zhang J, Wang DY. Simultaneously improving flame retardancy and dynamic mechanical properties of epoxy resin nanocomposites through layered copper phenylphosphate. *Compos Sci Technol*. 2018;154:136–44.
 15. Zhang J, Kong Q, Yang L, Wang DY. Few layered Co(OH)₂ ultrathin nanosheet-based polyurethane nanocomposites with reduced fire hazard: from eco-friendly flame retardance to sustainable recycling. *Green Chem*. 2016;10:3066–74.
 16. Zhang J, Kong Q, Wang DY. Simultaneously improving the fire safety and mechanical properties of epoxy resin with Fe-CNTs via large-scale preparation. *J Mater Chem A*. 2018;6:6376–86.
 17. Su D, Tang Z, Xie J, Bian Z, Zhang J, Yang D, Zhang D, Wang J, Liu Y, Yuan A, Kong Q. Co, Mn-LDH nanoneedle arrays grown on Ni foam for high performance supercapacitors. *Appl Surf Sci*. 2019;469:487–94.
 18. Basak S, Ali SW. Sodium tri-polyphosphate in combination with pomegranate rind extracts as a novel fire-retardant composition for cellulosic polymer. *J Therm Anal Calorim*. 2019;137:1233–47.
 19. Nawae S, Meesane J, Muensit N, Daengngam C. Layer-by-layer self-assembled films of silk fibroin/collagen/poly (diallyldimethylammonium chloride) as nucleating surface for osseointegration to design coated dental implant materials. *Mater Des*. 2018;160:1158–67.
 20. Kramer RK, Guimarães FEG, Carvalho AJF. Wood pulp fiber modification by layer-by-layer (LBL) self-assembly of chitosan/carboxymethyl cellulose complex: confocal microscopy characterization. *J Mol Liq*. 2019;273:368–73.
 21. Liu Y, Wang QQ, Jiang LM, Zhang CJ, Li ZF, Chen HQ, Zhu P. Effect of chitosan on the fire retardancy and thermal degradation properties of coated cotton fabrics with sodium phytate and APTES by LBL assembly. *J Anal Appl Pyrol*. 2018;135:289–98.
 22. Shariatnia Z. Pharmaceutical applications of chitosan. *Adv Colloid Interface*. 2019;263:131–94.
 23. Huang YF, Sun JJ, Wu DH, Feng XS. Layer-by-layer self-assembled chitosan/PAA nanofiltration membranes. *Sep Purif Technol*. 2018;207:142–50.
 24. Yang JC, Cao ZJ, Wang YZ, Schiraldi DA. Ammonium polyphosphate-based nanocoating for melamine foam towards high flame retardancy and anti-shrinkage in fire. *Polymer*. 2015;66:86–93.
 25. Maddalena L, Carosio F, Gomez J, Saracco G, Fina A. Layer-by-layer assembly of efficient flame retardant coatings based on high aspect ratio graphene oxide and chitosan capable of preventing ignition of PU foam. *Polym Degrad Stab*. 2018;152:1–9.
 26. Kundu CK, Wang W, Zhou S, Wang X, Sheng HB, Pan Y, Song L, Hu Y. A green approach to constructing multilayered nanocoating for flame retardant treatment of polyamide 66 fabric from chitosan and sodium alginate. *Carbohydr Polym*. 2017;166:131–8.
 27. Fang F, Zhang X, Meng Y, Gu Z, Bao C, Ding X, Li S, Chen X, Tian X. Intumescent flame retardant coatings on cotton fabric of chitosan and ammonium polyphosphate via layer-by-layer assembly. *Surf Coat Technol*. 2015;262:9–14.
 28. Pan H, Song L, Hu Y, Liew KM. An eco-friendly way to improve flame retardancy of cotton fabrics: layer-by-layer assembly of semi-biobased substance. *Energy Procedia*. 2015;75:174–9.
 29. Pan H, Wang W, Pan Y, Song L, Hu Y, Liew KM. Formation of self-extinguishing flame retardant biobased coating on cotton fabrics via layer-by-layer assembly of chitin derivatives. *Carbohydr Polym*. 2015;115:516–24.
 30. Alongi J, Carosio F, Malucelli G. Layer by layer complex architectures based on ammonium polyphosphate, chitosan and silica on polyester-cotton blends: flammability and combustion behavior. *Cellulose*. 2012;19:1041–50.
 31. Carosio F, Alongi J, Malucelli G. Layer by layer ammonium polyphosphate-based coatings for flame retardancy of polyester-cotton blends. *Carbohydr Polym*. 2012;88:1460–9.
 32. Khanal S, Zhang W, Ahmed S, Ali M, Xu S. Effects of intumescent flame retardant system consisting of tris (2-hydroxyethyl) isocyanurate and ammonium polyphosphate on the flame retardant properties of high-density polyethylene composites. *Compos Part A Appl Sci*. 2018;112:444–51.
 33. Turgut G, Dogan M, Tayfun U, Ozkoc G. The effects of POSS particles on the flame retardancy of intumescent polypropylene composites and the structure-property relationship. *Polym Degrad Stab*. 2018;149:96–111.
 34. Arjmandi R, Ismail A, Hassan A, Abu Bakar A. Effects of ammonium polyphosphate content on mechanical, thermal and flammability properties of kenaf/polypropylene and rice husk/polypropylene composites. *Constr Build Mater*. 2017;152:484–93.

35. Zhao L, Yan H, Fang Z, Wang J, Wang H. On the flameproof treatment of ramie fabrics using a spray-assisted layer-by-layer technique. *Polym Degrad Stab*. 2015;121:11–7.
36. Fang F, Xiao D, Zhang X, Meng Y, Cheng C, Bao C, Ding X, Cao H, Tian X. Construction of intumescent flame retardant and antimicrobial coating on cotton fabric via layer-by-layer assembly technology. *Surf Coat Technol*. 2015;276:726–34.
37. Yang JC, Liao W, Deng SB, Cao ZJ, Wang YZ. Flame retardation of cellulose-rich fabrics via a simplified layer-by-layer assembly. *Carbohydr Polym*. 2016;151:434–40.
38. Zhang D, Williams B, Shrestha S, Nasir Z, Becher E, Lofink B, Santos V, Patel H, Peng X, Sun L. Effects of ammonium polyphosphate content on mechanical, thermal and flammability properties of kenaf/polypropylene and rice husk/polypropylene composites. *J Colloid Interface Sci*. 2017;505:892–9.
39. Zheng Z, Qiang L, Yang T, Wang B, Cui X, Wang H. Preparation of microencapsulated ammonium polyphosphate with carbon source- and blowing agent-containing shell and its flame retardance in polypropylene. *J Polym Res*. 2014;21:443.
40. Jia Y, Lu Y, Zhang G, Liang Y, Zhang F. Facile synthesis of an eco-friendly nitrogen–phosphorus ammonium salt to enhance the durability and flame retardancy of cotton. *J Mater Chem A*. 2017;5:9970–81.
41. Liu L, Huang Z, Pan Y, Wang X, Song L, Hu Y. Finishing of cotton fabrics by multi-layered coatings to improve their flame retardancy and water repellency. *Cellulose*. 2018;25:4791–803.
42. Xu YJ, Wang J, Tan Y, Qi M, Chen L, Wang YZ. A novel and feasible approach for one-pack flame-retardant epoxy resin with long pot life and fast curing. *Chem Eng J*. 2018;337:30–9.
43. Zhao B, Liu DY, Liang WJ, Li F, Wang JS, Liu YQ. Bi-phase flame-retardant actions of water-blown rigid polyurethane foam containing diethyl-*N,N*-bis(2-hydroxyethyl) phosphoramidate and expandable graphite. *J Anal Appl Pyrol*. 2017;124:247–55.
44. Xu YJ, Chen L, Rao WH, Qi M, Guo DM, Liao W, Wang YZ. Latent curing epoxy system with excellent thermal stability, flame retardance and dielectric property. *Chem Eng J*. 2018;347:223–32.
45. Li ZF, Zhang CJ, Cui L, Zhu P, Yan C, Liu Y. Fire retardant and thermal degradation properties of cotton fabrics based on APTES and sodium phytate through layer-by-layer assembly. *J Anal Appl Pyrol*. 2017;123:216–23.

Publisher's Note Springer Nature remains neutral with regard to jurisdictional claims in published maps and institutional affiliations.